Spontaneous Ordering in Bulk GaN:Mg Samples

Z. Liliental-Weber,[1] M. Benamara,[1] J. Washburn,[1] I. Grzegory,[2] and S. Porowski[2]
[1]*Lawrence Berkeley National Laboratory, m/s 62/203, Berkeley, California 94720*
[2]*High Pressure Research Center "Unipress," Polish Academy of Sciences, Warsaw, Poland*
(Received 20 January 1999; revised manuscript received 2 June 1999)

Transmission electron microscopy evidence of spontaneous ordering in Mg-doped, bulk GaN crystals grown by a high pressure, high temperature process is reported for the first time. The ordering consists of Mg-rich planar defects formed on basal planes separated by 10 nm and occurs only for growth with $(000\bar{1})$ N polarity. The ordering leads to the formation of satellite diffraction spots dividing the (0001) reciprocal lattice distance into 20 parts. This "microsuperlattice" can be described as polytypoids comprised of planar defects with some characteristics of inversion domain boundaries.

PACS numbers: 68.35.Dv, 68.55.Ln, 61.16.Ch

Obtaining efficient p-type doping has been a continual challenge in GaN technology. At present, Mg is used for p-type doping in GaN with a thermal annealing activation step [1]. Mg-doped GaN and InGaN layers are essential components of light emitting diodes and lasers [2]. Despite the technical achievement, many aspects of Mg doping in GaN are not understood. For example, there are recent reports that Mg is not uniformly distributed in metal-organic chemical vapor deposition (MOCVD)-grown layers and has a tendency to diffuse to the film surface [3,4]. We report here evidence that, under certain growth conditions, Mg causes the formation of Mg-rich planar defects that form a superlatticelike array.

Mg-doped GaN crystals were grown by the high nitrogen pressure solution method [5] from a solution of liquid gallium containing 0.1–0.5 at. % Mg [6]. The crystals were grown at 1500–1600 °C and a N_2 pressure of 15 kbar for 100–150 h. Crystals in the form of hexagonal platelets approximately 80 μm thick and up to 8 mm across were formed [7]. p-type conductivity was not achieved; all crystals were highly resistive.

Bulk doping was achieved and secondary ion mass spectroscopy (SIMS) analysis shows a constant Mg distribution in the bulk of the sample at the level of 6×10^{19} cm^{-3}. Some increase in Mg concentration at the level of 2×10^{20} cm^{-3} was observed on both sides of the platelet sample. At the N-polar surface this increased concentration was visible up to 10 nm from the sample surface, but at the Ga-polar surface, only 2 nm. This observation of increased Mg concentration at the sample surface is similar to the earlier observation of GaN samples doped by Mg grown by MOCVD [3,4]. SIMS analysis also indicates the presence of oxygen and Si in the studied samples.

Transmission electron microscopy (TEM) was applied to study the microstructure of these samples. The sample polarity was determined by convergent beam electron diffraction (CBED) using the same methodology as Refs. [8,9]. Two different types of defects were observed in these samples: planar defects formed on the crystal side grown with N polarity and tetrahedral defects on the crystal side grown with Ga polarity (Fig. 1). This distinct difference in microstructure allows measurement of relative growth rates of these crystals for the two different polarities and shows that growth with N polarity is approximately 10 times slower than growth with opposite polarity. In this paper defects formed only on the N side will be discussed. The defects formed on the opposite side will be treated separately.

Cross-section TEM analysis [Fig. 2(a)] shows that the ordered structure forms on the $(000\bar{1})$ N polarity side of the crystal. Every 10 nm a layer with an enhanced contrast exists creating an equidistant layer structure. The formation of such an ordered superstructure has not to our knowledge been previously reported in GaN crystals. The defects maintain their c-plane orientation along the whole length of the plate shaped crystals (about 8 mm).

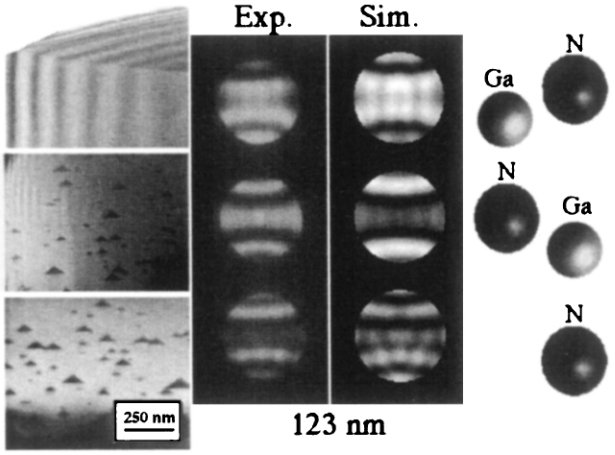

FIG. 1. Defect distribution for GaN:Mg together with an experimental and simulated CBED pattern showing crystal polarity. Note that defects with tetrahedral shape are present in the lower part of the crystal. In the upper part grown with N polarity planar defects are formed, but their contrast vanishes for this diffraction condition. These defects will be shown in Fig. 2.

 0031-9007/99/83(12)/2370(4)$15.00

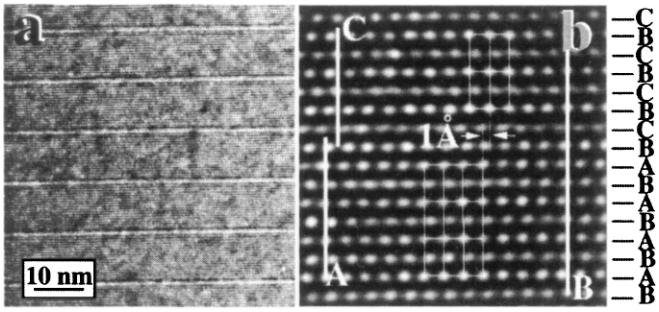

FIG. 2. (a) High magnification of the subsurface area grown in the N polar direction showing periodic arrangement of planar defects; (b) a magnified high resolution electron microscopy micrograph showing arrangement of atomic columns across the defect; *A*, *B*, and *C* show the stacking arrangement along the *c* axis. Note that the atom position indicated by *A* changes to the *C* position, but atoms on the *B* position remain unchanged on the two sides of the defect. However, some small deviations from the *B* position could be observed in the immediate vicinity of the defect.

The atomic stacking arrangement along the c axis can be described as *A*-*B*-*A*-*B*-*C*-*B*-*C* [Fig. 2(b)] with one sphalerite unit included, which is typical for the low energy stacking fault [9,10]. *A*, *B*, and *C* are the stacking positions (consisting of two atomic layers each) in the unit cell along the c axis. This defect introduces a $\frac{1}{3}[1\bar{1}00]$ displacement vector in the basal plane equivalent to about 1 Å, e.g., $\frac{1}{3}$ of 2.7 Å, which is the distance between $(1\bar{1}00)$ planes. This is in agreement with our tilting experiment for which defects go out of contrast for $g = [0002]$ and are in contrast for $g = [1\bar{1}00]$. In order to keep the same registry of a unit cell across the defect a $c/2$ shift needs to be considered in addition to the $\frac{1}{3}[1\bar{1}00]$ shift in the defect plane. This is equivalent to the removal of a basal layer followed by a slip of $\frac{1}{3}[1\bar{1}00]$ to reduce defect energy typical for the low energy stacking fault [9,10]. The same direction and the same magnitude of the displacement vector was observed for all defects. Fourier analysis of high resolution electron micrographs from the defects by integration of atomic columns along the $c/2$ atomic layers (0002) did not reveal any significant differences in lattice constant between the defect layer and surrounding layers suggesting that the $c/2$ distance on the defect remains unchanged.

Ordering close to the N polarity surface was observed in two out of five Mg-doped crystals studied here. However, in a third crystal further thinning uncovered bands of identical defects about 100 nm below the surface. This is an indication of incomplete ordering and suggests that the ordered structures will form only for certain critical growth conditions.

Figure 3 is a selective area diffraction pattern which shows the precise nature of the ordering. The presence of these regularly spaced planar defects leads to additional diffraction spots (see inset on the right hand side of Fig. 3) dividing the (0001) lattice distance (c^*) into 20 equal parts which corresponds to a $0.52 \times 20 = 10.4$ nm distance between the planar defects in real space. In addition to the satellite spots, (0001) and (0003) reflections are split (see inset on the left in Fig. 3) and the distance between the split reflections is almost equal to $c^*/20$ equivalent to the distance between ordered layers. A Fourier spectrum (not shown for lack of space) obtained from a high resolution image of an isolated defect confirms the splitting of forbidden reflections.

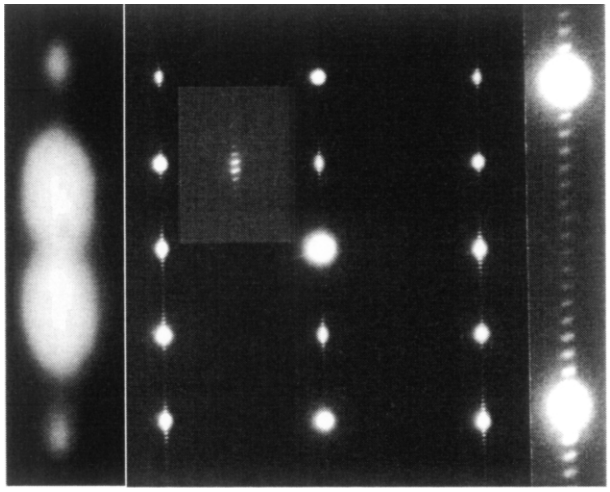

FIG. 3. Diffraction pattern obtained on the ordered area of the crystal grown in the N polar direction. Note satellite spots dividing (0001) into 20 equal spacings (see the inset to the right) and splitting of (0001) reflection (inset to the left). Note different intensity of split reflections compared to the satellite spots.

A dark field image (Fig. 4) obtained from the $[1\,1\,\bar{2}\,0]$ zone axis by placing either (0001) or $(000\bar{1})$ diffracted beams on the zone axis with a small objective aperture gives reverse contrast on the defects. The contrast is symmetric on the defect edges, e.g., white-white or dark-dark, and suggests that these defects are not simply stacking faults where asymmetric white-dark or dark-white contrast would be expected [11]. Both these observations, splitting

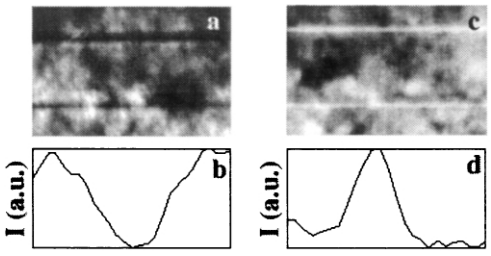

FIG. 4. Dark field image for planar defects obtained from the multibeam $[1\,1\,\bar{2}\,0]$ zone axis for (0001) and $(000\bar{1})$ reflections [(a) and (c)] together with the intensity profiles showing reverse contrast for $\pm g$ [(b) and (d), respectively] and symmetrical contrast on the two sides of the defect characteristic of an inversion boundary but not expected for a stacking fault.

of forbidden reflections and especially reverse contrast for $\pm g$ of a polar reciprocal lattice vector would indicate the presence of inversion domain boundaries (IDBs).

Energy dispersive x-ray (EDX) analysis (Fig. 5) with an electron beam size of the order of 1 nm was used to determine if the defects are Mg rich. The Mg K_α line overlaps with the shoulder of the Ga L_α peak; therefore, quantitative evaluation of the Mg peak is rather difficult. However, systematic comparison of the Mg K_α peak with the e-beam on the defects and between them (observed for the same acquisition time and the same sample thickness) gives us confidence that excess Mg is present on the defect. This is shown by the shaded area under the Mg peak on the inset in Fig. 5, where a spectrum obtained on the defect was superimposed on the spectrum obtained between the defects. Using the same procedure as for Mg, much higher N concentration was also observed on the defect (Fig. 5, inset—see shaded area under N peak) suggesting that the defects might be surrounded by nitrogen vacancies (V_N). The presence of Si and oxygen was also detected in the sample.

Why these equally spaced defects are formed only on the crystal side growing with N polarity is not easy to explain. The defects observed in these bulk GaN crystals are similar to defects that have been called polytypoids formed in AlN based crystals which are rich in oxygen (usually more than 1 at. %) [12–15]. One of the first descriptions of a polytypoid came from Jack [12] who proposed that polytypoids are arrays of stacking faults formed due to changes in the Al/N(O) ratio, e.g., metal (M) to nonmetal (X) ratio. Different types of polytypoids were observed depending on the M/X ratio. The smaller the ratio, the longer the period of a polytype (e.g., $M/X = 1/1 \rightarrow 2H$; $9/10 \rightarrow 27R$ [12]). However, later studies [13–15] showed that for an increase of oxygen content (about 0.75 at. %) an octahedral layer with metal in the center surrounded by oxygen (N) can be equally spaced forming a polytypoid. This octahedral layer (and the necessity for charge neutrality) produces a crystallographic inversion in the polar AlN, and then the MX_2 layer reinverts the lattice back to the previous polarity.

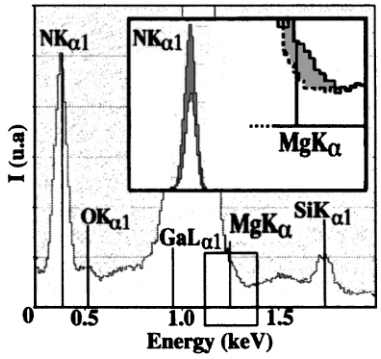

FIG. 5. EDX analysis on the defect area using a 1 nm probe. The inset shows differences in intensity for Mg and N when the beam is placed on the defect (shaded) and outside the defect (dotted lines).

Defects in bulk GaN:Mg appear to be similar to those in AlN; however, the oxygen concentration in these crystals is always much below 1 at. % [16]. In addition, the observed defects occur only on the crystal side grown with N polarity. Our EDX studies show higher Mg and N concentration on the defects than between them (Fig. 5); therefore, addition of Mg appears to be responsible for the formation of these defects. Similar oxygen concentration (5×10^{19} cm^{-3}) in undoped crystals does not lead to their formation [8]. Oxygen presence, however, together with Mg might stabilize these defects. It is clear from this study that polytypoids are formed in GaN:Mg due to Mg segregation. It is known that Mg together with Al, N, O, and Si form polytypoids [12]; therefore, similar defects might be formed with Ga instead of Al. The fact that ordering is not observed for all studied samples, and especially the occurrence of incomplete ordering in one sample, suggests that the ordering will occur only for certain very specific growth conditions. The sudden change observed in one of the crystals suggests that a change of N pressure may have taken place (since other parameters such as growth temperature would be expected to remain constant). If N concentration does change this would lead to a change of M/X ratio, assuming constant Mg concentration.

Recent angle dependent x-ray studies of GaN:Mg grown by the same method [17] showed that Mg is distributed on the basal planes and Mg forms bonds exclusively with N atoms inclined to the c planes, and not with N atoms along the c axis. Theoretical calculations by Bungaro *et al.* [18] show a different Mg arrangement on the two polar GaN surfaces and predict segregation of Mg on the N-polar surface. Our results are therefore the first experimental proof that such segregation is taking place. To our knowledge, however, there are no theoretical predictions of an ordered arrangement for Mg in GaN, but one could expect the formation of planar defects for growth with N polarity based on this theoretical work [18]. Since growth on the N-polar surface is much slower compared to growth on the Ga polar surface, then once a planar defect is formed it should propagate on the basal plane during further crystal growth.

What are these defects? The shift of $\frac{1}{3}[1\bar{1}00] + c/2$ is consistent with the model that these polytypoids are equally spaced stacking faults as originally described by Jack [12]. However, the formation and the splitting of forbidden reflections and the reverse contrast under a dark field multibeam condition using polar reciprocal ± 0001 reflections strongly suggest that these planar defects contain IDB pairs. This would be similar to the results obtained earlier for AlN:O [13,15]. However, as in AlN:O [15] partial ordering is taking place in some GaN:Mg crystals and large thicknesses of defect free

hexagonal layers are sometimes inserted between ordered regions. Since these changes are very abrupt we believe that slight changes in N pressure during the crystal growth might occur causing the local composition change.

In summary, this TEM study shows, for the first time, that ordered planar Mg rich defects can be formed in Mg-doped GaN crystals during growth in the N polar direction. The defects have characteristics suggesting that they are closely spaced inversion boundary pairs. Regular spacing of these defects with a separation of only 10 nm was observed. This "microsuperlattice" leads to satellite diffraction spots dividing the (0001) reciprocal lattice distance into 20 parts. Segregation of Mg in the planar defects would explain why p-type doping of GaN using Mg is difficult.

This work was supported by the Director, Office of Basic Science, Materials Science Division, U.S. Department of Energy, under Contract No. DE-AC03-76SF00098. The use of the facility at the National Center for Electron Microscopy at E. O. Lawrence Berkeley National Laboratory is greatly appreciated. Z. L. W. thanks J. Ager for a careful reading of this manuscript and W. Swider for wonderful TEM sample preparation.

[1] S. Nakamura, N. Iwasa, M. Senoh, and T. Mukai, Jpn. J. Appl. Phys. **31**, 1258 (1992).
[2] S. Nakamura, in Proceedings of the 24th International Symposium on Compound Semiconductors, San Diego, CA, 1997 (to be published).
[3] M. E. Lin, G. Xue, L. Zhou, J. E. Greene, and H. Morkoc, Appl. Phys. Lett. **63**, 932 (1993).
[4] S. Guha, N. A. Bojarczuk, and F. Cardone, Appl. Phys. Lett. **71**, 1685 (1997).
[5] I. Grzegory, J. Jun, M. Bockowski, St. Krukowski, M. Wroblewski, B. Lucznik, and S. Porowski, J. Phys. Chem. Solids **56**, 639 (1995).
[6] S. Porowski, M. Bockowski, B. Lucznik, I. Grzegory, M. Wroblewski, H. Teisseyre, M. Leszczynski, E. Litwin-Staszewska, T. Suski, P. Trautman, K. Pakula, and J. M. Baranowski, Acta Phys. Pol. A **92**, 958 (1997).
[7] Z. Liliental-Weber, M. Benamara, J. Washburn, I. Grzegory, and S. Porowski, Mater. Res. Soc. Symp. Proc. (to be published).
[8] Z. Liliental-Weber, C. Kisielowski, S. Ruvimov, Y. Chen, J. Washburn, I. Grzegory, M. Bockowski, J. Jun, and S. Porowski, J. Electron. Mater. **25**, 1545 (1996).
[9] Z. Liliental-Weber, M. Benamara, O. Richter, W. Swider, J. Washburn, I. Grzegory, S. Porowski, J. W. Yang, and S. Nakamura, Mater. Res. Soc. Symp. Proc. **512**, 363 (1998).
[10] D. Hull and D. J. Bacon, *Introduction to Dislocations*, International Series on Materials Science and Technology Vol. 37 (Pergamon Press, Oxford, New York, 1984), 3rd ed., pp. 112–121.
[11] D. B. Williams and C. B. Carter, in *Transmission Electron Microscopy* (Plenum Press, New York, 1996), pp. 386–390.
[12] K. H. Jack, J. Mater. Sci. **11**, 1135 (1976).
[13] Y. Yan, M. Terauchi, and M. Tanaka, Philos. Mag. A **77**, 1027 (1998).
[14] R. A. Youngman, A. D. Westwood, and M. R. McCartney, Mater. Res. Soc. Symp. Proc. **319**, 45 (1994).
[15] A. D. Westwood, R. A. Youngman, M. R. McCartney, and A. N. Cormack, J. Mater. Res. **10**, 1270 (1995).
[16] C. Wetzel, T. Suski, J. W. Ager III, E. R. Weber, E. E. Haller, S. Fischer, B. K. Meyer, P. J. Molnar, and P. Perlin, Phys. Rev. Lett. **78**, 3023 (1997).
[17] K. Lawniczak-Jablonska, T. Suski, J. Libera, J. Kachniarz, P. Lagarde, R. Cortes, and I. Grzegory (unpublished).
[18] C. Bungaro, K. Rapcewicz, and J. Bernholc, Phys. Rev. B **59**, 9771 (1999).